Synergistic effect and mechanisms of ultrasound and AlOOH suspension on Al hydrolysis for hydrogen production

Wei-Zhuo Gai [a,*], Shuang Tian [a,b], Ming-Hao Liu [a], Xianghui Zhang [a], Zhen-Yan Deng [c]

[a] College of Physics and Electronic Information & Henan Key Laboratory of Electromagnetic Transformation and Detection, Luoyang Normal University, Luoyang 471934, China
[b] College of Physics Science and Technology, Nanjing Normal University, Nanjing 210023, China
[c] Energy Materials & Physics Group, Department of Physics, Shanghai University, Shanghai 200444, China

A B S T R A C T

Ultrasound can accelerate and change the reaction process and is widely used in the field of hydrogen production and storage. In this study, ultrasound (US) and AlOOH suspension (AH) are used to promote hydrogen production from Al hydrolysis. The results indicate that both US and AH greatly shorten the induction time and enhance the hydrogen production rate and yield. The promoting effect of US and AH on Al hydrolysis originates from the acoustic cavitation effect and catalytic effect, respectively. When AH is used in combination with US, Al hydrolysis has the best hydrogen production performance and the hydrogen yield can reach 96.6 % within 1.2 h, because there is a synergistic effect on Al hydrolysis between AH and US. Mechanism analyses reveal that the micro-jets and local high temperature environment arising from acoustic cavitation improve the catalytic activity of AlOOH, while the suspended AlOOH particles enhance the cavitation effect of US. This work provides a novel and feasible method to promote hydrogen production from Al hydrolysis.

1. Introduction

Hydrogen is an eye-catching and promising energy carrier due to its remarkable advantages of extensive sources, high calorific value and pollution-free [1]. Hydrogen energy can be converted into electrical energy with low pollution emission and high efficiency through a fuel cell process [2]. The wide application of fuel cells can alleviate the increasingly serious energy and environmental crisis to a certain extent, while its commercialization process still faces some difficult issues, including the development of cost competitive hydrogen production technologies and efficient and safe storage methods [3], especially for portable small-sized fuel cell.

As is known, ultrasound can accelerate and control the chemical reaction, improve the yield and change the reaction process. During the past decade, ultrasonic technology has been widely used in the field of hydrogen production and storage and achieved great progress [4–7]. For example, Hiroi et al. demonstrated that ultrasonic irradiation could effectively promote the hydrolysis of MgH_2 and enhance hydrogen yield [8]. A similar result was obtained in the hydrolysis of NH_3BH_3, which showed that ultrasonic irradiation affected the structure of Co-B catalyst and increased the hydrogen production rate by 38 % [9]. Escobar-

Alarcón et al. developed a new hydrogen generation approach, in which hydrogen was produced through laser ablating Mg, Al, Ti and Al-Mg alloy under ultrasonic field. Ultrasonic irradiation increased the hydrogen yield by about 100 % [10,11]. Wang et al. applied ultrasound to hydrogen production of perovskite $CH_3NH_3PbI_3$ via a synergistic piezophotocatalysis. Ultrasonic vibration produced an internal electric field by exerting periodic strain on $CH_3NH_3PbI_3$, which promoted the separation of charge carriers and enhanced hydrogen generation [12].

In fact, water sonolysis is an effective and widely studied way to produce hydrogen [4]. When water is irradiated by ultrasound, a sonolysis process induced by acoustic cavitation occurs [13,14],

$$H_2O \leftrightarrow H^{\bullet} + {}^{\bullet}OH \tag{1}$$

$$H^{\bullet} + {}^{\bullet}OH \leftrightarrow H_2 + O \tag{2}$$

$$H^{\bullet} + O_2 \leftrightarrow HO_2 \tag{3}$$

$$H^{\bullet} + HO_2 \leftrightarrow H_2 + O_2. \tag{4}$$

During the sonolysis process, hydrogen is produced through the recombination of $H^{\bullet}$ and $^{\bullet}OH$ originated from the dissociation of water molecule. The sonochemical hydrogen production process is affected by
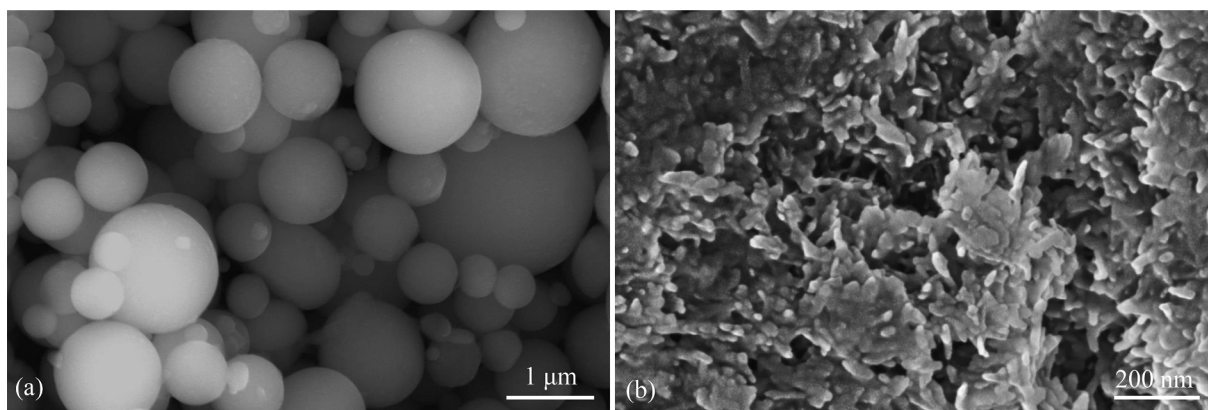
Fig. 1. SEM micrographs of (a) as-received pure Al powder and (b) AlOOH powder obtained through filtering and drying AH.

many factors, including dissolved gases, bubble temperature, ultrasonic frequency and intensity, suspended particles, catalysts, etc. [15–18]. The hydrogen production rate of water sonolysis is relative slow (1.05 × 10^{-3} μmol/h at ultrasonic frequency of 20 kHz and power of 30 W) [14], limiting its application.

Metal Al has the advantages of low price, abundant, high gravimetric hydrogen storage density and convenient storage and transportation, endowing it great potential in the field of in situ hydrogen production [19]. Al hydrolysis can produce 1.25 L/g-Al hydrogen with high purity, which can provide hydrogen for portable small-sized fuel cell. Furthermore, Al can be stored and transported in a more convenient way than hydrogen, and can release hydrogen through hydrolysis when needed, avoiding the hydrogen storage problem and solving the hydrogen source issue of small-sized fuel cell. Park et al. [20] developed a 50 W hydrogen generator based on Al hydrolysis, which can stably supply hydrogen for polymer electrolyte membrane fuel cell (PEMFC). Wang et al. [21] also proved the feasibility of Al hydrolysis for PEMFC. They designed a safe and simple hydrogen generator, which produced hydrogen through Al hydrolysis in NaOH solution. This hydrogen generator using 6 g Al can stably operate PEMFC under 500 mA for 5 h. However, the dense oxide film forming on Al surface owing to exposure to air or humid environment hinders the direct reaction of Al with water, resulting in a long induction time and slow hydrogen production rate of Al hydrolysis in water.

Recently, some researchers discovered that aluminum oxides and hydroxides could be used as catalysts to accelerate Al hydrolysis [22–24]. For example, Newell et al. [25] demonstrated that amorphous aluminum hydroxide prepared through urea hydrolysis could speed up Al hydrolysis and promote hydrogen generation. Prabu et al. [26] confirmed that aluminum hydroxide prepared by ethanol precipitation method could catalyze Al hydrolysis. However, the catalytic activity of aluminum hydroxide is poor owing to the agglomeration in the preparation process. Moreover, the byproduct of Al hydrolysis reaction covers Al surface and repassivates Al at the later stage of reaction, which hinders the transport of water molecules and reduces the hydrogen production rate [27]. To improve the catalytic activity of aluminum hydroxide and inhibit the repassivation of Al by byproduct, in this research, AlOOH suspension instead of AlOOH powder was used to catalyze Al hydrolysis with ultrasonic assistance, and the synergetic promotion mechanisms of AlOOH and ultrasound were revealed.

2. Materials and methods

Al powder with the average particle size of 0.95 μm (Henan Yuanyang Powder Technology Co., ltd., China), $NaAlO_2$ and HCl with analytical reagent grade (Sinopharm Chemical Reagent Co., ltd., China) were used as received in this research.

AlOOH suspension was prepared by hydrothermal method using

$NaAlO_2$ as Al source. Simply, the diluted HCl solution was added drop wise into 130 ml of solution containing 4.6 mmol $NaAlO_2$ through a PTFE burette. In order to promote the reaction and inhibit the agglomeration of AlOOH particles, the titration process was carried out continuously in an ultrasonic field (100 W, 40 kHz) until the pH value reached 9 ± 0.2. In this case, a white homogeneous suspension was obtained,

$$NaAlO_2 + HCl \rightarrow AlOOH\downarrow + NaCl. \tag{5}$$
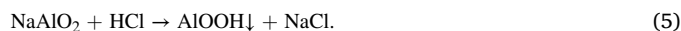
Subsequently, the above suspension was transferred into a Teflon-lined autoclave and hydrothermal treated at 150 °C for 10 h. Finally, the obtained suspension was cooled to room temperature and dispersed for 10 min by ultrasonic treatment. The AlOOH suspension was labeled as AH and used to promote Al hydrolysis.

The hydrogen production tests by Al hydrolysis were performed in a double-necked flask under ultrasonic radiation (US), which was generated by an ultrasonic cleaner (Type: KQ-500DE, power 500 W (adjustable), frequency 40 kHz, China). In each test, 150 ml of AlOOH suspension with the concentration of 20 wt% (the weight fraction of AlOOH in Al powder + AlOOH) and 1.0 g of Al powder were used. The ultrasonic power was 200–500 W (power density: 19.0–47.6 W/L) and the reaction temperature was 30–50 °C. In order to eliminate the temperature rise caused by ultrasound and keep a constant reaction temperature, the water in ultrasonic cleaner was changed every 10 min. Water displacement method was used to measure the volume of hydrogen generated from Al hydrolysis [5], and hydrogen yield (α) can be calculated.

$$\alpha = \frac{V_{H_2}}{V_0} \times 100\% \tag{6}$$

where V_{H_2} is the volume of hydrogen at time t and V_0 is the theoretical hydrogen volume. As the hydrogen production rate of water sonolysis process (3.9 × 10^{-5} ml/min at ultrasonic frequency of 20 kHz and power of 30 W) was much slower than that of Al hydrolysis in this work (average rate was about 2.0–13.0 ml/min) [14], the hydrogen produced from water sonolysis process was not considered. The crystal structures and morphologies of Al powder and its byproduct were analyzed using X-ray diffractometer (XRD, D8 Advance, Germany) and scanning electron microscope (SEM, Sigma 500/VP, Germany), respectively.

3. Results and discussion

3.1. Effect of AlOOH suspension and ultrasound

Fig. 1 presents the morphologies of original Al powder and AlOOH powder obtained through filtering and drying AH. Al particles have spherical shape and range from tens of nanometers to several micrometers (Fig. 1a). AlOOH grains are very fine and have rod-like structures
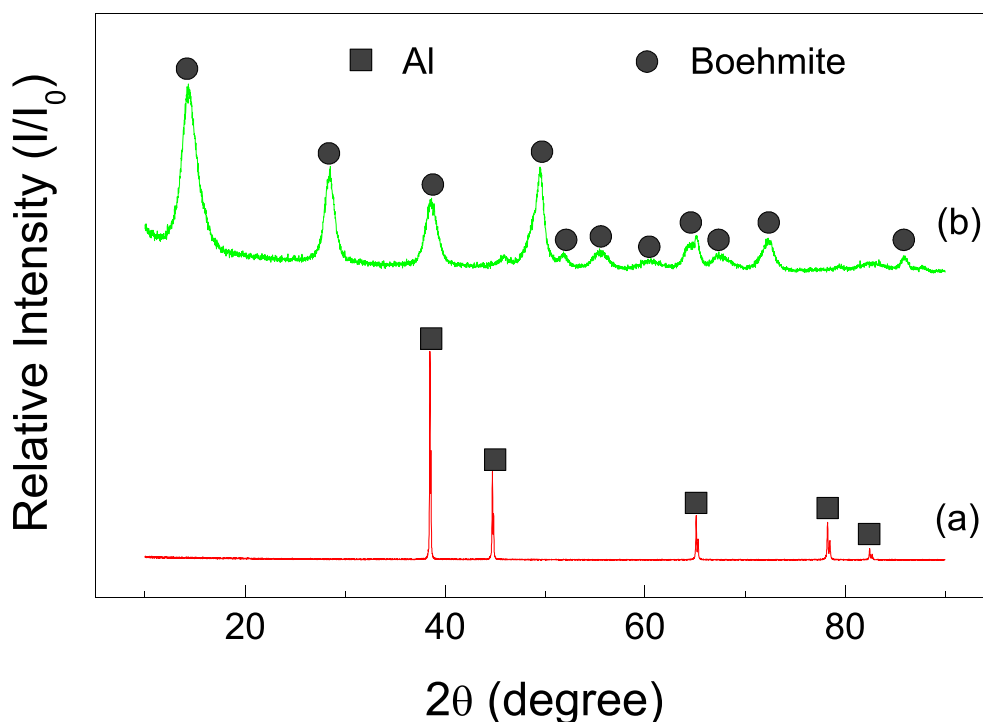
Fig. 2. X-ray patterns of (a) as-received pure Al powder and (b) AlOOH powder obtained through filtering and drying AH.
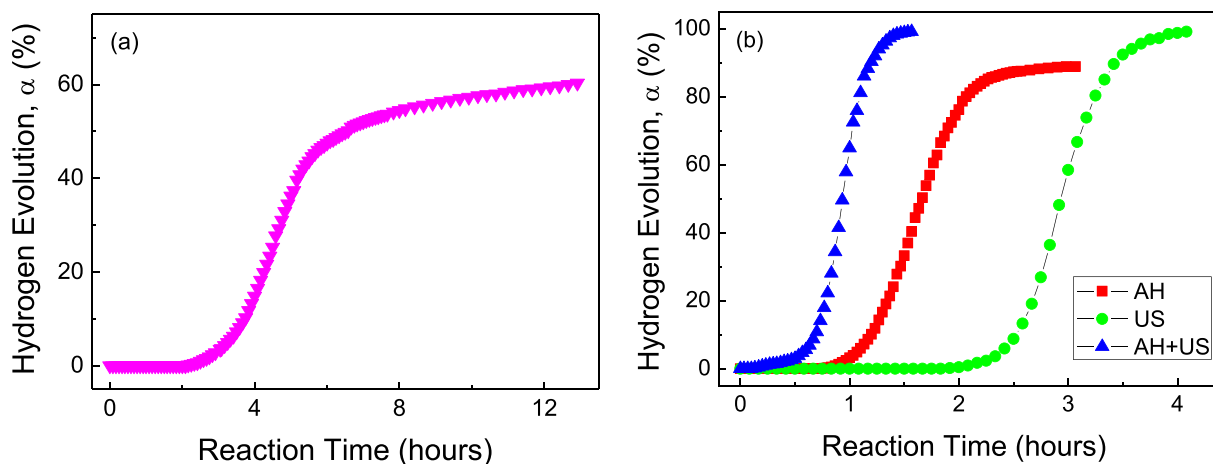
Fig. 3. Hydrogen evolution curves of Al hydrolysis at 40 °C in (a) deionized water and (b) deionized water or AH under different conditions, where "US" means that Al hydrolysis reaction was conducted under ultrasonic field.

with 20–30 nm in diameter and 70–120 nm in length, but there are many agglomerates, which were produced in the filtering and drying processes of AH (Fig. 1b). Fig. 2 exhibits the XRD patterns of original Al powder and AlOOH powder. Obviously, only five diffraction peaks assigned to pure Al were observed, implying that it has a high purity. For AlOOH powder, only one crystalline phase (i.e. boehmite) was detected. The diffraction peaks are wide, meaning that AlOOH grains are fine, which is consistent with the result of Fig. 1b.

Fig. 3a gives the hydrogen evolution curve of Al hydrolysis at 40 °C in deionized water. As can be seen, pure Al powder could continuously hydrolyze with deionized water to produce hydrogen, while it needs a long induction time of 2.42 h before hydrogen release due to the hindering effect of passive oxide film on Al surface. Fig. 3b shows the hydrogen evolution curves of Al hydrolysis at 40 °C under different conditions. Both ultrasound (US) and AlOOH suspension (AH) promoted Al hydrolysis and improved hydrogen production performances. After

introducing US into Al hydrolysis, the induction time decreased from 2.42 to 1.83 h, and the maximum hydrogen production rate (v_{max}) increased from 6.80 to 33.00 ml·min^{-1}·g^{-1}-Al. Comparing with US, AH had a better promoting effect on Al hydrolysis, and the induction time was shortened to 0.73 h. However, the hydrogen yield of AH was 88.90 %, which was lower than that of US (99.14 %). The possible reason is that the byproduct layer thickened and repassivated Al at the later stage of Al hydrolysis. When US was used, US can break the byproduct layer and inhibit the repassivation of Al, resulting in a higher hydrogen yield. When AH was used in combination with US (AH + US), Al hydrolysis had the best hydrogen production performance. The hydrogen yield can reach 96.6 % within 1.2 h, and the induction time was only 0.17 h. The promoting effect of reaction conditions on Al hydrolysis is in the order of AH + US > AH > US, indicating that AH + US is an effective and feasible method to promote Al hydrolysis.

As is known, ultrasound can stir and disperse suspension, which may
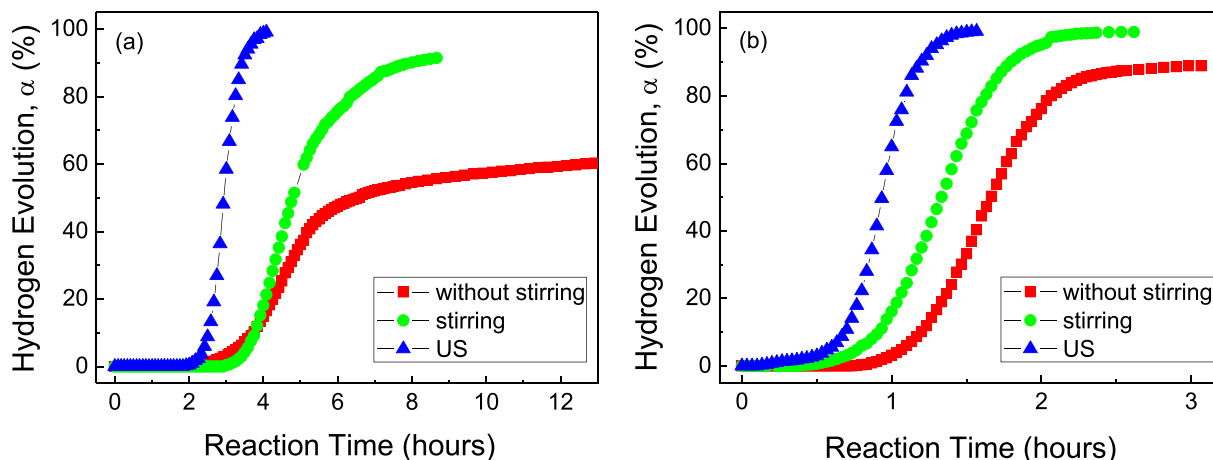
Fig. 4. Hydrogen evolution curves of Al hydrolysis at 40 °C in (a) deionized water and (b) AH with and without stirring or under ultrasonic field.

Table 1
Hydrogen production data of Al hydrolysis at 40 °C under different conditions.

Reaction conditions	Induction time (h)	v_{max} (ml·min^{-1}·g^{-1}-Al)[a]	Hydrogen yield (%)	Reaction time (h)
DIW[b], without stirring	2.42	6.80	60.32	12.92
DIW + stirring	2.92	11.20	91.49	8.67
DIW + US	1.83	33.00	99.14	4.08
AH, without stirring	0.73	28.00	88.90	3.07
AH + stirring	0.37	30.00	98.92	2.62
AH + US	0.17	66.00	99.14	1.57

[a] v_{max} is the maximum hydrogen production rate of Al hydrolysis.
[b] DIW is deionized water.

Fig. 5. Hydrogen evolution curves of Al hydrolysis at 40 °C in AH under ultrasonic field with different power density.

be the reason why US promotes Al hydrolysis. To clarify this issue, Al hydrolysis tests in deionized water and AH under three dispersion conditions, i.e. without stirring, stirring and US were conducted, as shown in Fig. 4 and Table 1 summarizes the specific hydrogen production data. For deionized water, stirring increased induction time from 2.42 to 2.92 h and enhanced hydrogen yield from 60.32 % to 91.49 %. There is almost no inorganic anions and cations in deionized water, but it still contains trace organic species, such as organic acids, which can react with passive oxide film on Al surface and form Al-organics complexes, inhibiting the hydration process of passive oxide film and prolonging the induction time [28,29]. The concentration of total organic carbon (TOC) in deionized water used in this work is 1.20 mg/L. Due to the low ionic strength and TOC concentration, the movement velocity of organic species using concentration gradient as driving force was very slow. When stirring was used, the organic species moved fast, resulting in the rapid formation of Al-organics complexes on Al surface. Therefore, stirring increased the induction time of Al hydrolysis. However, when US was introduced into Al hydrolysis, the induction time decreased rather than increased. It can be inferred that US has other effects besides dispersion. The dynamics of Al hydrolysis can be described using shrinking core model [30]. At the initial and later stages, Al hydrolysis was controlled by surface chemical reaction and H_2O molecule diffusion in the byproduct layer, respectively [27]. With the process of reaction, the byproduct layer increased gradually. Furthermore, some hydroxide byproduct was easy to form aggregates when no stirring was used. In this case, the diffusion resistance of H_2O molecules increased and Al repassivation occurred, which is the reason why Al hydrolysis without stirring has low hydrogen production rate and yield. When stirring was used, it can accelerate the diffusion of H_2O molecule
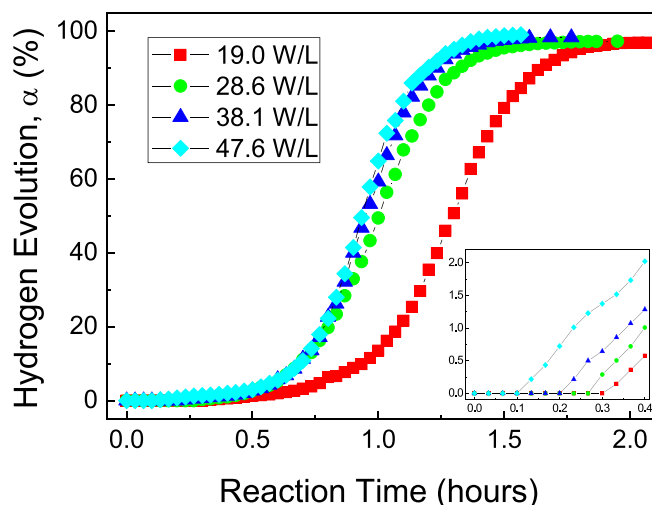
and inhibit the agglomeration of byproduct, so stirring increased the hydrogen production rate and yield. Comparing with stirring, Al hydrolysis had much higher hydrogen production rate and yield when US was used, which further indicates US has other effects besides dispersion.

As shown in Fig. 4b, the effect of dispersion conditions on Al hydrolysis in AH was similar to that in deionized water excepting that stirring shortened induction time. This is reasonable, because stirring enhanced the contact chance of Al with AlOOH, which improved the promoting effect of AH and decreased induction time. Furthermore, AlOOH can adsorb the trace organic species in deionized water, inhibiting the formation of Al-organics complexes on Al surface. Both stirring and US improved hydrogen production performance of Al hydrolysis in AH. Stirring and US shortened induction time from 0.73 to 0.37 and 0.17 h and increased v_{max} from 28.00 to 30.00 and 66.00 ml·min^{-1}·g^{-1}-Al, respectively. Clearly, the promoting effect of US was much higher that of stirring, implying that US has other effects besides dispersion.

3.2. Effect of ultrasonic condition

The influence of ultrasound on chemical reaction mainly originates from cavitation effect, which is closely related to ultrasonic conditions, such as power density, ultrasonic temperature, etc. Fig. 5 illustrates the hydrogen production performance of Al hydrolysis in AH under
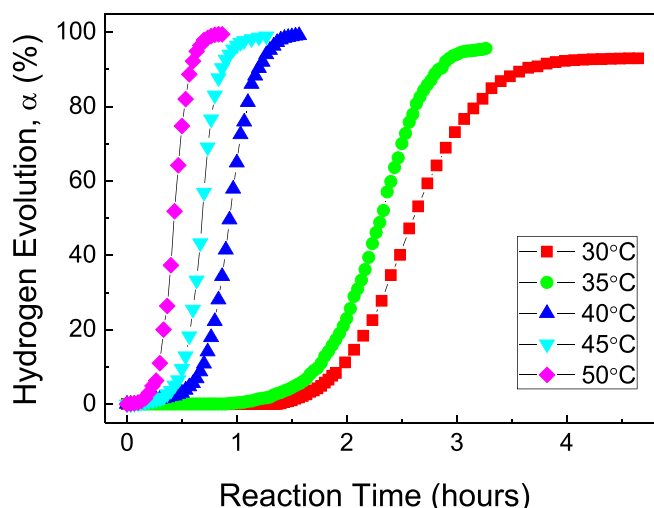
Fig. 6. Hydrogen evolution curves of Al hydrolysis at different temperatures in AH under ultrasonic field, where the ultrasonic power density is 47.6 W/L.

ultrasonic field with different power density. Obviously, increasing ultrasonic power density accelerated Al hydrolysis. When the power density increased from 19.0 to 47.6 W/L, the induction time shortened from 0.30 to 0.17 h and v_{max} increased from 42.50 to 66.00 ml·min^{-1}·g^{-1}-Al. The hydrogen production performance was improved significantly when increasing the power density from 19.0 to 28.6 W/L, because increasing power density improved cavitation intensity [31]. However, the hydrogen production performance had slight improvement when further increasing power density from 28.6 to 47.6 W/L, implying that the ultrasonic cavitation effect tends to be saturated.

Fig. 6 presents the hydrogen evolution curves of Al hydrolysis at different temperature under the condition of AH + US. When temperature was 30 °C, the hydrogen production performance of Al hydrolysis

was poor. The induction time was as high as 1.37 h and v_{max} was only 19.60 ml·min^{-1}·g^{-1}-Al. When raising temperature from 30 °C to 50 °C, the hydrogen production performance was greatly improved. At 50 °C, there was no induction time and the hydrogen yield can reach 97.9 % within 0.7 h. v_{max} was as high as 102.50 ml·min^{-1}·g^{-1}-Al, which was comparable with the result of Al hydrolysis in alkaline solution [32]. Raising temperature made reactant molecules in a more excited state, which enhanced the contact chance of Al with AlOOH and increased the diffusion rate of H$_2$O molecules in the byproduct layer, improving Al hydrolysis reaction dynamics [23,33]. Moreover, increasing temperature was beneficial to the formation of acoustic cavitation bubbles, which further shortened the induction time and accelerated Al hydrolysis.

3.3. Physicochemical mechanisms

It is widely known that there is a passive oxide film with thickness of 3–5 nm on Al particle surface [34], blocking the direct contact of inner Al with water. Therefore, the passive film needs undergo a hydration process before hydrogen release from Al hydrolysis, which explains the origin of induction time [35,36]. Fig. 7 exhibits the schematic representations of hydration process of passive film on Al surface under different reaction conditions. For Al hydrolysis in deionized water (Fig. 7a), it takes a long time to complete hydration process of the passive film, which is the cause for longer induction time. According to Fig. 3b, US and AH shortened induction time and accelerated Al hydrolysis, implying that US and AH can promote the hydration process of passive film. When AH was used in combination with US, the promoting mechanisms of AH + US on Al hydrolysis consisted of the following three aspects.

(1) Role of US

When ultrasound is introduced into a liquid environment, it can generate many acoustic cavitation bubbles. These cavitation bubbles will undergo an acoustic cavitation process, which
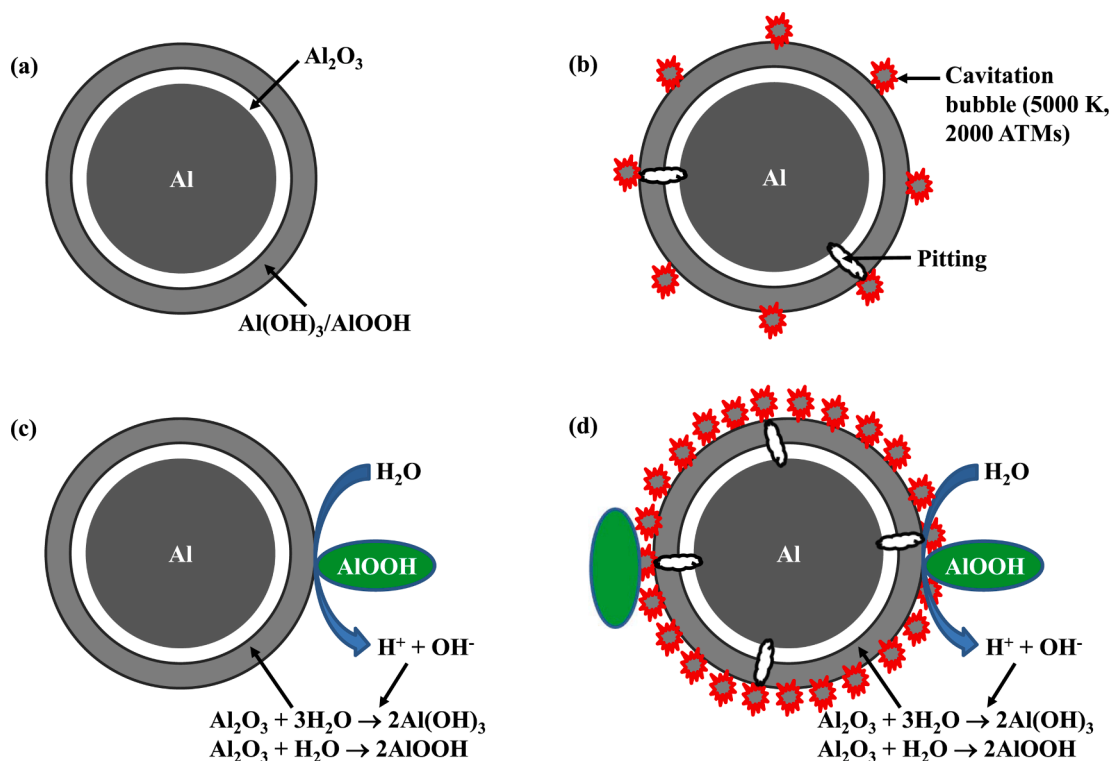
Fig. 7. Schematic representations of hydration process of the passive film on Al particle surface under different reaction conditions: (a) in deionized water, (b) US, (c) AH and (d) AH + US.

includes three consecutive stages: formation, growth and implosive collapse [37]. The promoting effect of US on Al hydrolysis is mainly attributed to acoustic cavitation effect, as shown in Fig. 7b. During cavitation process, the implosive collapse of cavitation bubbles can create many local hot spots, which provide an unusual environment with temperature of > 5000 K and pressure of > 2000 ATMs for chemical reaction [14]. In addition, implosive collapse also generates micro-jets and shock waves with the velocity of hundreds meters per second [38]. The local high temperature environment accelerates the hydration process of passive film and shortens the induction time. Furthermore, the micro-jets and shock waves can destroy and remove the hydration byproduct ($Al(OH)_3$ or $AlOOH$) of passive film in hot spots, resulting in the formation of pits. This phenomenon is called pitting of Al [35], therefore Al hydrolysis under the condition of US is a combination of pitting and uniform corrosion. These pits provide transport channels for H_2O molecules and accelerate the transport process, which further shortens the induction time.

After induction time, US also plays an important role in promoting Al hydrolysis. On one hand, the local high temperature environment improves Al hydrolysis reaction dynamics and increases the diffusion rate of H_2O molecules in the byproduct layer, leading to a significant increase in hydrogen production rate. On the other hand, the micro-jets and shock waves accelerate the diffusion of H_2O molecules in byproduct and inhibit the agglomeration of byproduct, preventing Al from repassivation. This is the reason why US greatly increases hydrogen production rate and yield (Fig. 4 and Tabel 1).

(2) Role of AH

The promoting effect of AH on Al hydrolysis derives mainly from the catalytic effect of AlOOH [23], as shown in Fig. 7c. AlOOH has a high surface reactivity and is usually used as catalyst or catalyst support, because it has a defect spinel structure, in which some cation sites are vacant [39]. AlOOH behaves as a "reactive sponge" and can store and release H_2O molecules. When H_2O molecules arrive at AlOOH surface, they are chemisorbed and dissociated into H^+ and OH^- ions [40]. In AH, when Al particles come into contact with AlOOH grains, the H^+ and OH^- ions dissociated from H_2O molecules can easily hydrate with the passive film on Al surface, promoting the hydration process. This explains the reason why AH significantly shortens the induction time. Furthermore, the suspended AlOOH particles can act as crystallization nuclei in Al hydrolysis, preventing Al from repassivation [41]. Therefore, AH accelerates Al hydrolysis and enhances hydrogen yield.

(3) Synergistic effect of AH and US

There is a synergistic effect on Al hydrolysis between AH and US, as shown in Fig. 7d. Firstly, the micro-jets and shock waves originated from acoustic cavitation enhance the contact chance of Al with AlOOH, improving the catalytic activity of AlOOH. Meanwhile, the local high temperature environment further improves the catalytic effect of AlOOH on Al hydrolysis. Additionally, US inhibits the agglomeration of AlOOH, increasing the amount of AlOOH nuclei for crystallization of Al hydrolysis byproduct. Secondly, the suspended AlOOH particles can enhance the cavitation effect and increase the cavitation bubbles [15,42]. In this case, more pits are produced on Al surface, accelerating Al hydrolysis and increasing hydrogen yield.

For US or AH, only mechanism (1) or mechanism (2) is effective in Al hydrolysis, respectively, which is the reason why the hydrogen production performance of Al hydrolysis under the condition of AH + US is much better than that of AH or US (Fig. 3 and Table 1).
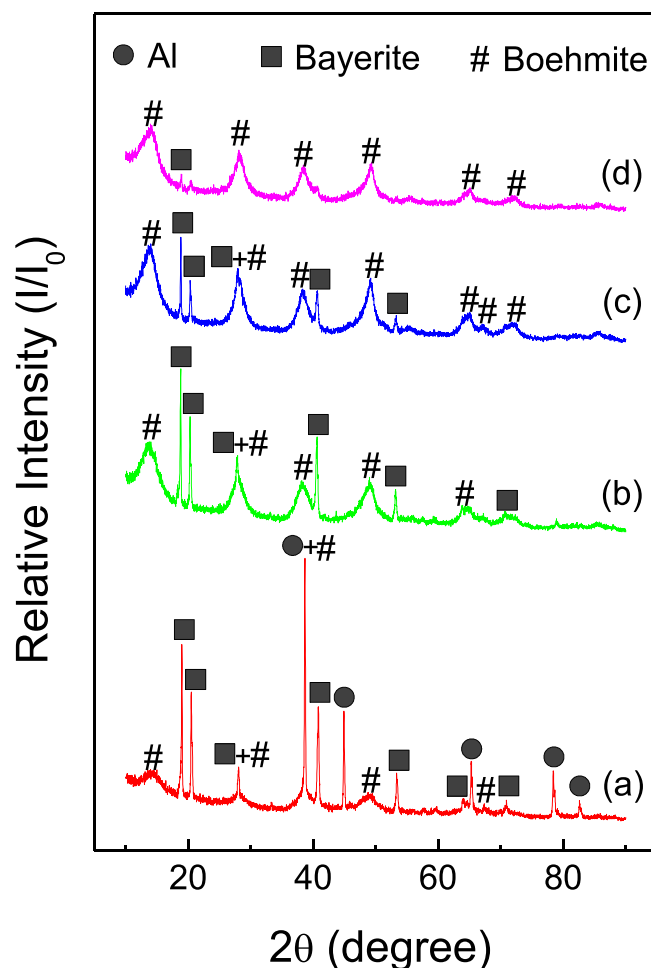
Fig. 8. X-ray patterns of the byproducts of Al hydrolysis under different conditions: (a) in deionized water, (b) US, (c) AH and (d) AH + US.

3.4. Reaction byproduct

Fig. 8 demonstrates the XRD patterns of byproducts of Al hydrolysis under different reaction conditions. Obviously, all the byproducts under different reaction conditions contained two phases, i.e. bayerite and boehmite. Therefore, the equations of Al hydrolysis can be written.

$$2Al + 6H_2O \rightarrow 2Al(OH)_3 + 3H_2\uparrow \qquad (7)$$

$$2Al + 4H_2O \rightarrow 2AlOOH + 3H_2\uparrow \qquad (8)$$

Interestingly, the contents of bayerite and boehmite in byproducts under different conditions were obvious different, suggesting that the phase compositions of byproducts depended heavily on reaction conditions. For deionized water, most of the byproduct was bayerite and only small part was boehmite (Fig. 8a). Besides, the diffraction peaks of Al were also detected, indicating that Al was not completely hydrolyzed in deionized water. This is reasonable, because hydrogen yield of Al hydrolysis in deionized water was only 60.32 % (Fig. 3a). Under the conditions of US, AH and AH + US, the diffraction peaks of bayerite decreased, meaning that the content of bayerite decreased while the content of boehmite increased. The content of boehmite in byproducts was in the order of AH + US > AH > US > deionized water. For AH + US, the phase in byproduct was mainly boehmite, which can be explained as follow. On one hand, the local high temperature environment originated from acoustic cavitation was beneficial to the formation of boehmite, because boehmite had a higher forming temperature than bayerite [27,37]. On the other hand, the suspended AlOOH particles in AH can
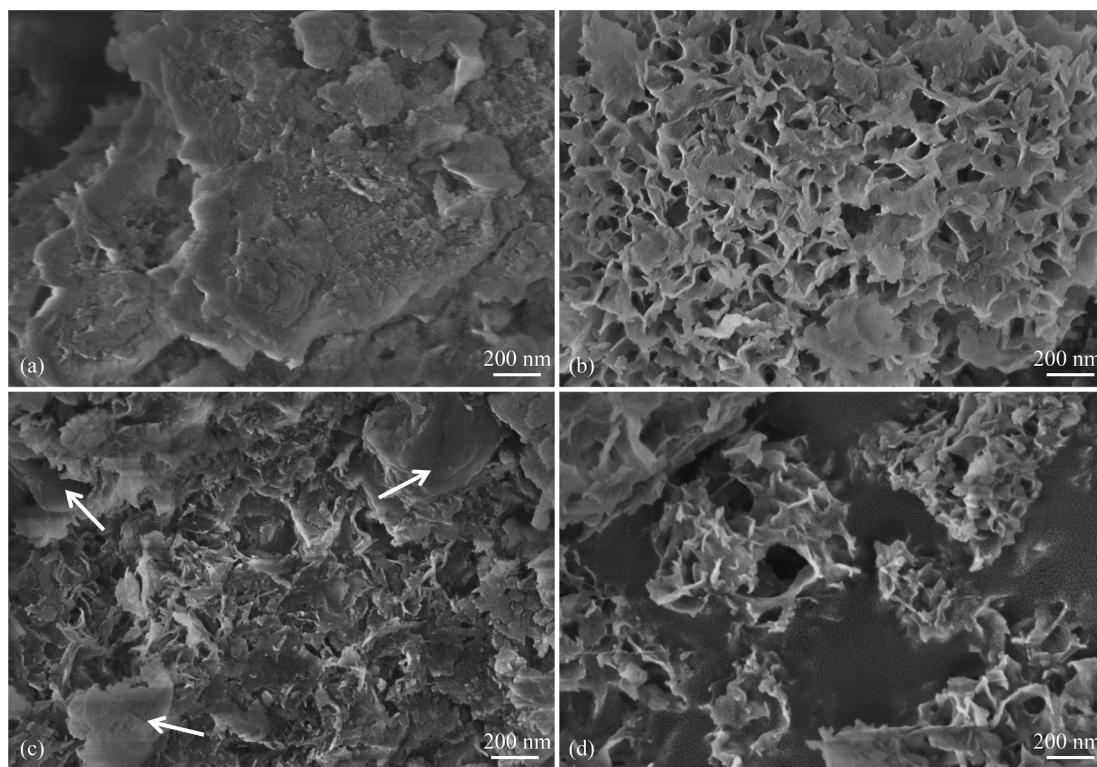
Fig. 9. SEM micrographs of the byproducts of Al hydrolysis under different conditions: (a) in deionized water, (b) US, (c) AH and (d) AH + US.

act as crystallization nuclei in Al hydrolysis, promoting the formation of AlOOH.

Fig. 9 gives the SEM micrographs of byproducts of Al hydrolysis under different conditions. For deionized water, the byproduct had a lump structure and there were many large agglomerates (Fig. 9a). Under the conditions of US, AH and AH + US, the byproducts had a flower-like structure and the grains were fine. This is due to the fact that the rapid hydrogen production resulted in the breakage of byproduct layers on Al surface. There were still some agglomerates in byproduct under the condition of AH (arrows in Fig. 9c), while almost no agglomerates were observed in byproduct under the condition of US and AH + US (Fig. 9b and d). This can be explained by the fact that the micro-jets and shock waves arising from acoustic cavitation can effectively break the agglomerates in byproduct [43].

4. Conclusions

In this work, the effect of US and AH on Al hydrolysis was systematically investigated. Both US and AH significantly promoted Al hydrolysis and enhanced hydrogen production performance due to the acoustic cavitation effect of US and catalytic effect of AH. US and AH shortened the induction time from 2.42 to 1.83 and 0.73 h and increased v_{max} from 6.80 to 33.00 and 28.00 ml·min^{-1}·g^{-1}-Al, respectively. When AH was used in combination with US (AH + US), Al hydrolysis exhibited the best hydrogen production performance owing to the synergistic effect between AH and US. At 50 °C, there was no induction time and v_{max} was as high as 102.50 ml·min^{-1}·g^{-1}-Al. A possible promoting mechanism of AH + US was proposed, which revealed that the micro-jets and local high temperature environment arising from acoustic cavitation enhanced the catalytic activity of AH, meanwhile, the suspended AlOOH particles in AH enhanced the cavitation effect of US. Furthermore, the hydrogen production performance of Al hydrolysis can be controlled through adjusting the ultrasonic power density and temperature. This study provides an effective and feasible way to promote Al hydrolysis for hydrogen production.

CRediT authorship contribution statement

Wei-Zhuo Gai: Conceptualization, Writing – original draft, Formal analysis, Supervision. **Shuang Tian:** Methodology, Formal analysis, Investigation. **Ming-Hao Liu:** Investigation, Data curation. **Xianghui Zhang:** Validation. **Zhen-Yan Deng:** Writing – review & editing.

Declaration of Competing Interest

The authors declare that they have no known competing financial interests or personal relationships that could have appeared to influence the work reported in this paper.

Data availability

The data that has been used is confidential.

Acknowledgements

References

[1] A.M. Kler, E.A. Tyurina, Y.M. Potanina, A.S. Mednikov, Estimation of efficiency of using hydrogen and aluminum as environmentally-friendly energy carriers, Int. J. Hydrogen Energy 40 (2015) 14775–14783, https://doi.org/10.1016/j.ijhydene.2015.09.041.

[2] Z.Y. Deng, J.M.F. Ferreira, Y. Sakka, Hydrogen-generation materials for portable applications, J. Am. Ceram. Soc. 91 (2008) 3825–3834, https://doi.org/10.1111/j.1551-2916.2008.02800.x.

[3] X.N. Huang, T. Gao, X.L. Pan, D. Wei, C.J. Lv, L.S. Qin, Y.X. Huang, A review: feasibility of hydrogen generation from the reaction between aluminum and water for fuel cell applications, J. Power Sources 229 (2013) 133–140, https://doi.org/10.1016/j.jpowsour.2012.12.016.

[4] S.S. Rashwan, I. Dincer, A. Mohany, B.G. Pollet, The sono-hydro-gen process (ultrasound induced hydrogen production): challenges and opportunities, Int. J.

Hydrogen Energy 44 (2019) 14500–14526, https://doi.org/10.1016/j.ijhydene.2019.04.115.

[5] W.Z. Gai, X.H. Zhang, K.X. Sun, Z.Y. Deng, Hydrogen generation from Al-water reaction promoted by M-B/γ-Al₂O₃ (M = Co, Ni) catalyst, Int. J. Hydrogen Energy 44 (2019) 24377–24386, https://doi.org/10.1016/j.ijhydene.2019.07.203.

[6] H.Y. Hafeez, S.K. Lakhera, M. Ashokkumar, B. Neppolian, Ultrasound assisted synthesized of reduced grapheme oxide (rGO) supported In-VO₄-TiO₂ nanocomposite for efficient hydrogen production, Ultrason. Sonochem. 53 (2019) 1–10, https://doi.org/10.1016/j.ultsonch.2018.12.009.

[7] G. Yang, J.L. Wang, Ultrasound combined with dilute acid pretreatment of grass for improvement of fermentative hydrogen production, Bioresource Technol. 275 (2019) 10–18, https://doi.org/10.1016/j.biortech.2018.12.013.

[8] S. Hiroi, S. Hosokai, T. Akiyama, Ultrasonic irradiation on hydrolysis of magnesium hydride to enhance hydrogen generation, Int. J. Hydrogen Energy 36 (2011) 1442–1447, https://doi.org/10.1016/j.ijhydene.2010.10.093.

[9] A.K. Figen, B. Coskuner, A novel perspective for hydrogen generation from ammonia borane (NH₃BH₃) with Co-B catalysts: "ultrasonic hydrolysis", Int. J. Hydrogen Energy 38 (2013) 2824–2835, https://doi.org/10.1016/j.ijhydene.2012.12.067.

[10] L.E. Alarcón, J.L. Iturbe-GarcÍa, F. González-Zavala, D.A. Solis-Casados, R. Pérez-Hernández, E. Haro-Poniatowski, Hydrogen production by ultrasound assisted liquid laser ablation of Al, Mg and Al-Mg alloys in water, Appl. Surf. Sci. 478 (2019) 189–196, https://doi.org/10.1016/j.apsusc.2019.01.213.

[11] L.E. Alarcón, J.L. Iturbe-GarcÍa, F. González-Zavala, D.A. Solis-Casados, R. Pérez-Hernández, E. Haro-Poniatowski, Hydrogen production by laser irradiation of metals in water under an ultrasonic field: A novel approach, Int. J. Hydrogen Energy 44 (2019) 1579–1585, https://doi.org/10.1016/j.ijhydene.2018.11.158.

[12] M. Wang, Y. Zuo, J. Wang, Y. Wang, X. Shen, B. Qiu, L. Cai, F. Zhou, S.P. Lau, Y. Chai, Remarkably enhanced hydrogen generation of organolead halide perovskites via piezocatalysis and photocatalysis, Adv. Energy Mater. 9 (2019) 1901801, https://doi.org/10.1002/aenm.201901801.

[13] S. Merouani, O. Hamdaoui, Y. Rezgui, M. Guemini, Mechanism of the sonochemical production of hydrogen, Int. J. Hydrogen Energy 40 (2015) 4056–4064, https://doi.org/10.1016/j.ijhydene.2015.01.150.

[14] S.S. Rashwan, I. Dincer, A. Mohany, An investigation of ultrasonic based hydrogen production, Energy 205 (2020), 118006, https://doi.org/10.1016/j.energy.2020.118006.

[15] R. Sasikala, O.D. Jayakumar, S.K. Kulshreshtha, Enhanced hydrogen generation by particles during sonochemical decomposition of water, Ultrason. Sonochem. 14 (2007) 153–156, https://doi.org/10.1016/j.ultsonch.2006.06.005.

[16] Y.F. Wang, D. Zhao, H.W. Ji, G.L. Liu, C.C. Chen, W.H. Ma, H.Y. Zhu, J.C. Zhao, Sonochemical hydrogen production efficiency catalyzed by Au/TiO₂, J. Phys. Chem. C 114 (2010) 17728–17733, https://doi.org/10.1021/jp105691v.

[17] S. Merouani, O. Hamdaoui, Y. Rezgui, M. Guemini, Computational engineering study of hydrogen production via ultrasonic cavitation in water, Int. J. Hydrogen Energy 41 (2016) 832–844, https://doi.org/10.1016/j.ijhydene.2015.11.058.

[18] S.S. Rashwan, I. Dincer, A. Mohany, A unique study on the effect of dissolved gases and bubble temperatures on the ultrasonic hydrogen (sonohydrogen) production, Int. J. Hydrogen Energy 45 (2020) 20808–20819, https://doi.org/10.1016/j.ijhydene.2020.05.022.

[19] Y.Q. Wang, W.Z. Gai, X.Y. Zhang, H.Y. Pan, Z.X. Cheng, P.G. Xu, Z.Y. Deng, Effect of storage environment on hydrogen generation by the reaction of Al with water, RSC Adv. 7 (2017) 2103–2109, https://doi.org/10.1039/C6RA25563A.

[20] J.T. Park, X.R. Xu, J. Wang, X.J. Zhu, A small-scale and portable 50 W PEMFC system that automatically generates hydrogen from a mixture of Al, CaO, NaOH and sodium CMC in water without external power supply, Int. J. Hydrogen Energy 38 (2013) 10511–10518, https://doi.org/10.1016/j.ijhydene.2013.05.177.

[21] E.D. Wang, P.F. Shi, C.Y. Du, X.R. Wang, A mini-type hydrogen generator from aluminum for proton exchange membrane fuel cells, J. Power Sources 181 (2008) 144–148, https://doi.org/10.1016/j.jpowsour.2008.02.088.

[22] H.T. Teng, T.Y. Lee, Y.K. Chen, H.W. Wang, G.Z. Cao, Effect of Al(OH)₃ on the hydrogen generation of aluminum-water system, J. Power Sources 219 (2012) 16–21, https://doi.org/10.1016/j.jpowsour.2012.06.077.

[23] W.Z. Gai, C.S. Fang, Z.Y. Deng, Hydrogen generation by the reaction of Al with water using oxides as catalysts, Int. J. Energy Res. 38 (2014) 918–925, https://doi.org/10.1002/er.3093.

[24] Y. Yang, W.Z. Gai, Z.Y. Deng, J.G. Zhou, Hydrogen generation by the reaction of Al with water promoted by an ultrasonically prepared Al(OH)₃ suspension, Int. J.

Hydrogen Energy 39 (2014) 18734–18742, https://doi.org/10.1016/j.ijhydene.2014.09.085.

[25] A. Newell, K.R. Thampi, Novel amorphous aluminum hydroxide catalysts for aluminum-water reactions to produce H₂ on demand, Int. J. Hydrogen Energy 42 (2017) 23446–23454, https://doi.org/10.1016/j.ijhydene.2017.04.279.

[26] S. Prabu, S.C. Hsu, J.S. Lin, H.W. Wang, Rapid hydrogen generation from the reaction of aluminum powders and water using synthesized aluminum hydroxide catalysts, Top. Catal. 61 (2018) 1633–1640, https://doi.org/10.1007/s11244-018-0970-x.

[27] W.Z. Gai, W.H. Liu, Z.Y. Deng, J.G. Zhou, Reaction of Al powder with water for hydrogen generation under ambient condition, Int. J. Hydrogen Energy 37 (2012) 13132–13140, https://doi.org/10.1016/j.ijhydene.2012.04.025.

[28] W.Z. Gai, Z.Y. Deng, Effect of trace species in water on the reaction of Al with water, J. Power Sources 245 (2014) 721–729, https://doi.org/10.1016/j.jpowsour.2013.07.042.

[29] P. Pommerenk, G.C. Schafran, Adsorption of inorganic and organic ligands onto hydrous aluminum oxide: evaluation of surface charge and the impacts on particle and NOM removal during water treatment, Environ. Sci. Technol. 39 (2005) 6429–6434, https://doi.org/10.1021/es050087u.

[30] L. Soler, A.M. Candela, J. Macanás, M. Muñoz, J. Casado, In situ generation of hydrogen from water by aluminum corrosion in solutions of sodium aluminate, J. Power Sources 192 (2009) 21–26, https://doi.org/10.1016/j.jpowsour.2008.11.009.

[31] H. Zhang, J.H. Zhang, C.Y. Zhang, F. Liu, D.B. Zhang, Degradation of C.I. Acid Orange 7 by the advanced Fenton process in combination with ultrasonic irradiation, Ultrason. Sonochem. 16 (2009) 325–330, https://doi.org/10.1016/j.ultsonch.2008.09.005.

[32] H.Q. Yang, H.L. Zhang, R.C. Peng, S.S. Zhang, X.R. Huang, Z.D. Zhao, Highly efficient hydrolysis of magnetic milled powder from waste aluminum (Al) cans with low-concentrated alkaline solution for hydrogen generation, Int. J. Energy Res. 43 (2019) 4797–4806, https://doi.org/10.1002/er.4621.

[33] A. Bolt, I. Dincer, M. Agelin-Chaab, Experimental study of hydrogen production process with aluminum and water, Int. J. Hydrogen Energy 45 (2020) 14232–14244, https://doi.org/10.1016/j.ijhydene.2020.03.160.

[34] F.J. Martin, G.T. Cheek, W.E. O'Grady, P.M. Natishan, Impedance studies of the passive film on aluminum, Corros. Sci. 47 (2005) 3187–3201, https://doi.org/10.1016/j.corsci.2005.05.058.

[35] B.C. Bunker, G.C. Nelson, K.R. Zavadil, J.C. Barbour, F.D. Wall, J.P. Sullivan, C. F. Windisch, M.H. Engelhardt, D.R. Baer, Hydration of passive oxide films on aluminum, J. Phys. Chem. B 106 (2002) 4705–4713, https://doi.org/10.1021/jp013246e.

[36] Z.Y. Deng, J.M.F. Ferreira, Y. Tanaka, J.H. Ye, Physicochemical mechanism for the continuous reaction of γ-Al₂O₃ modified aluminum powder with water, J. Am. Ceram. Soc. 90 (2007) 1521–1526, https://doi.org/10.1111/j.1551-2916.2007.01546.x.

[37] T. Chave, S.I. Nikitenko, D. Granier, T. Zemb, Sonochemical reactions with mesoporous alumina, Ultrason. Sonochem. 16 (2009) 481–487, https://doi.org/10.1016/j.ultsonch.2008.12.015.

[38] K.S. Suslick, Mechanochemistry and sonochemistry: concluding remarks, Faraday Discuss. 170 (2014) 411–422, https://doi.org/10.1039/C4FD00148F.

[39] K. Sohlberg, S.J. Pennycook, S.T. Pantelides, Hydrogen and the structure of the transition aluminas, J. Am. Chem. Soc. 121 (1999) 7493–7499, https://doi.org/10.1021/ja991098o.

[40] A. Ionescu, A. Allouche, J.P. Aycard, M. Rajzmann, F. Hutschka, Study of γ-alumina surface reactivity: adsorption of water and hydrogen sulfide on octahedral aluminum sites, J. Phys. Chem. B 106 (2002) 9359–9366, https://doi.org/10.1021/jp020145n.

[41] L. Soler, A.M. Candela, J. Macanás, M. Muñoz, J. Casado, Hydrogen generation by aluminum corrosion in seawater promoted by suspensions of aluminum hydroxide, Int. J. Hydrogen Energy 34 (2009) 8511–8518, https://doi.org/10.1016/j.ijhydene.2009.08.008.

[42] N.H. Ince, G. Tezcanli, R.K. Belen, I.G. Apikyan, Ultrasound as a catalyzer of aqueous reaction systems: the state of the art and environmental applications, Appl. Catal. B-Environ. 29 (2001) 167–176, https://doi.org/10.1016/S0926-3373(00)00224-1.

[43] P. Ding, A.W. Pacek, De-agglomeration of goethite nano-particles using ultrasonic comminution device, Powder Technol. 187 (2008) 1–10, https://doi.org/10.1016/j.powtec.2007.12.016.